

Thermal Analysis of a Finned Thermosyphon for Heat Exchanger Applications

V.M. Aguiar¹, G.A. Bartmeyer¹, L. Krambeck¹, P.H.D. Santos², T. Antonini Alves¹

¹Federal University of Technology - Paraná, 84.016-210, PONTA GROSSA, Brazil

Email: viniciusmarrone@hotmail.com, gabartmeyer@hotmail.com, larikrambeck@hotmail.com, thiagoaalves@utfpr.edu.br

²Federal University of Technology - Paraná, 80.230-901, CURITIBA, Brazil

Email: psantos@utfpr.edu.br

Abstract— A thermosyphon is a gravity-assisted heat pipe used to improve the heat transfer in several applications. In this paper, a thermal analysis of a finned thermosyphon for heat exchanger applications was experimentally researched. The thermosyphon was manufactured from a copper tube the external diameter of 9.45 mm, the inner diameter of 7.75 mm, and a total length of 200 mm. The working fluid used was water with a filling ratio of 40% of the evaporator volume. The condenser was cooled by air forced convection, the adiabatic section was insulated with fiberglass and the evaporator was heated by an electrical resistor. Experimental tests were performed to a heat load from 5 up to 50W at vertical position (evaporator above condenser). As a result of the research, the thermosyphon operated satisfactorily to the tested position. Also, the finned thermosyphon obtained better thermal performance than the un-finned condenser, proving the effectiveness of the fin application.

Keywords— fins, thermal analysis, thermosyphon.

I. INTRODUCTION

A thermosyphon is a gravity-assisted heat pipe used to improve the heat transfer in several applications [1]. The main feature of a thermosyphon is the use of vaporization latent heat to transmit heat at high rates over considerable distances with small temperature decrease. Its advantages are flexibility, simple construction, and easy control with no external pumping power [2].

Thermosyphons have three regions with distinct roles in their operation. These regions are evaporator, adiabatic section, and condenser. The evaporator, the lower region of the tube, is heated by a hot source and the working fluid undergoes an evaporation process. This steam, because of the pressure difference, moves to the colder region (condenser). In this region, the steam generated in the evaporator loses energy as heat and is condensed. The working fluid in liquid state flows back to the evaporator by gravity, closing the cycle. The adiabatic section is located between the evaporator and the condenser. In this section, there is no heat transfer between the

thermosyphon and the environment. In some cases, the adiabatic section is absent [3]. A schematic diagram of the thermosyphon operating principle is shown in Fig. 1. More details of the thermosyphons can be found in [2]-[6].

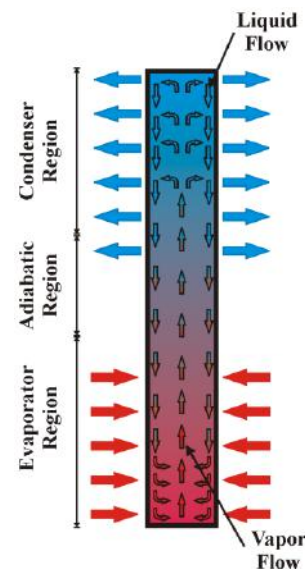


Fig. 1: Sketch of the operating principle of a thermosyphon.

Thermosyphons can be widely applied in the industrial environment. An application example is the heat recovery in a hot exhaust gas system by preheating air in heat exchangers of boilers. Furthermore, the heat transfer in heat exchangers can be improved by the use of fins, which can be coupled to the evaporator and/or the condenser of the thermosyphons [7].

In this context, a thermal analysis of a finned thermosyphon was experimentally researched. Due to its geometric characteristics, the thermosyphon can be applied in the preheating air of heat exchangers.

II. METHODOLOGY

The methodology for manufacture (cleaning, assembly, the tightness test, the evacuation process, and the filling with the working fluid), experimental tests, and thermal

analysis of the finned thermosyphon was based taking into the consideration the instructions of [8]-[10].

2.1 Characteristics of Developed Thermosyphon

A copper tube ASTM B-75 Alloy 122 with an outer diameter of 9.45 mm, an inner diameter of 7.75 mm, and a length of 200 mm was used to manufacture the thermosyphon. The thermosyphon has an evaporator of 80 mm in length, an adiabatic region of 20 mm in length and, a condenser of 100 mm in length. Aluminum fins were installed in the condenser region. Figure 2 presents the manufactured thermosyphon. The working fluid used was water with a filling ratio of 40% of the evaporator volume. Table 1 shows the main features of the finned thermosyphon.



Fig. 2: Finned thermosyphon

Table.1: Main characteristics of the finned thermosyphon

| Characteristics | Thermosyphon |
|------------------------------|--------------|
| Inner diameter [mm] | 7.75 |
| Outer diameter [mm] | 9.45 |
| Evaporator [mm] | 80 |
| Adiabatic section [mm] | 20 |
| Condenser [mm] | 100 |
| Working fluid | Water |
| Filling ratio [%] | 40 |
| Volume of working fluid [mL] | 1.60 |

2.2 Experimental Apparatus

The experimental apparatus used for the experimental tests, shown in Fig. 3, is composed of a power supply unit (AgilentTM U8002A), a data logger (AgilentTM 34970A with 20 channels), a laptop (DellTM), an uninterruptible power supply (NHSTM), a universal support, and a fan (UltrarTM).

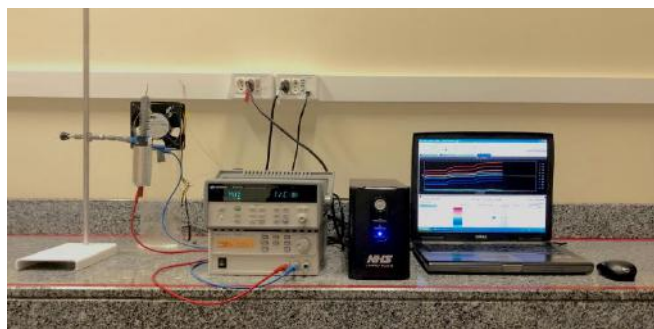


Fig. 3: Experimental Apparatus

For the evaluation of the thermal performance of the finned thermosyphon, K-type thermocouples Omega EngineeringTM were used. They were fixed on the outer surface of the tube by a thermosensitive adhesive strip KaptonTM. As shown in Fig. 4, there were three thermocouples in the evaporator ($T_{evap,1}$, $T_{evap,2}$, and $T_{evap,3}$), one thermocouple in the adiabatic section (T_{adiab}) and four thermocouples in the condenser ($T_{cond,1}$, $T_{cond,2}$, $T_{cond,3}$, and $T_{cond,4}$) in finned thermosyphon.

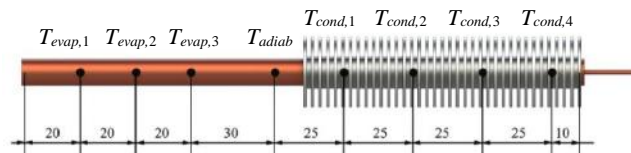


Fig. 4: Thermocouple positions [mm]

The heating system of the evaporator was conducted by power dissipation in a power strip resistor Omega EngineeringTM. To ensure that the generated heat by Joule effect was transmitted to the evaporator, an aeronautic thermal insulation and a layer of polyethylene were installed in this region. A fiberglass tape was used in adiabatic section as heat insulation between the support and the thermosyphon. The cooling system using air forced convection consisted of a fan in the condenser region. As mentioned above, to intensify the cooling, aluminum fins were installed in the condenser region.

2.3 Experimental Procedure

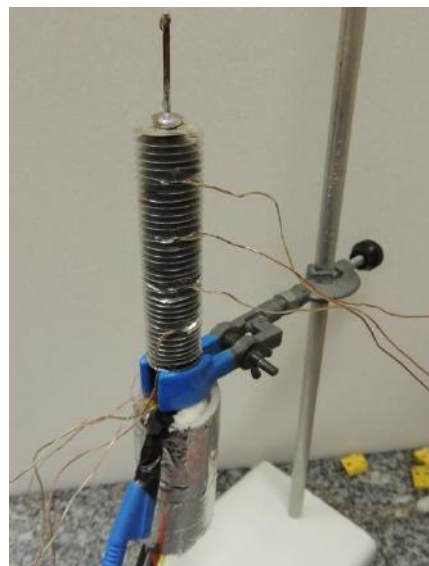


Fig. 5: Finned thermosyphon at the vertical position.

To ensure the best results and the repeatability of experimental tests, the ambient temperature was maintained at $19.0^{\circ}\text{C} \pm 1.0^{\circ}\text{C}$ by the thermal conditioning system CarrierTM. The finned thermosyphon was tested at the vertical position (evaporator above the condenser).

Figure 5 shows the finned thermosyphon test. The fan was turned on, positioned correctly in the condenser region and set at a speed of 5.0 m/s with a combined error of ± 0.2 m/s. The data acquisition system was turned on, and the temperatures measured by the thermocouples.

The power supply unit was turned on and adjusted to the dissipation power desired. The initial load was 5W and, after approximately 15 minutes, the thermocouples showed stationary values. The load increment of 5W was made up to 50W or until the maximum average temperature of the thermosyphon reached the critical temperature (150 °C), where the melting of the materials could happen. Data were acquired every ten seconds, recorded on the laptop by the software Agilent™ Benchlink Data Logger 3.

The experimental uncertainties are associated to the K-type thermocouples, the data logger, and the power supply unit. The experimental temperature uncertainty is estimated to be approximately ± 1.27 °C and a thermal load was $\pm 1\%$. For the uncertainties determination, the Error Propagation Method described by [11] was used.

III. DATA REDUCTION

The thermal performance of the finned thermosyphon was analyzed according to the operating temperature and the thermal resistance. The operating temperature analyzed was the temperature of the adiabatic region. The total thermal resistance, R_{th} , of a thermosyphon can be defined as the difficulty of the device to carry heat. The higher the thermal resistance, the greater the difficulty is in transporting heat from the system [12]. The total thermal resistance can be calculated by

$$R_{th} = \frac{\Delta T}{q} = \frac{(T_{evap} - T_{cond})}{q}, \quad (1)$$

where, q is the heat transfer capability of the finned thermosyphon, T_{evap} and T_{cond} are the average wall temperature of the evaporator and the condenser, respectively.

IV. RESULTS AND DISCUSSION

The experimental results regarding the thermal performance of the finned thermosyphon are presented considering the vertical position. The experimental tests were repeated three times and the errors were compared taking into account the difference between the mean values were less than 0.5 °C. Tests were performed to a heat load varying from 5 to 50 W. Figure 6 shows the temperature distribution as a function of time for the finned thermosyphon.

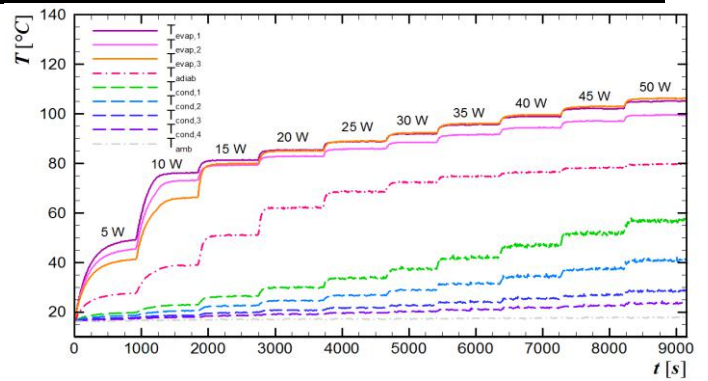


Fig. 6: Temperature distribution versus time

The temperature distribution in function of the finned thermosyphon length for the heat loads is presented in Fig. 7. The evaporator temperatures remain close to each other for the heat loads. The condenser temperatures reduce gradually.

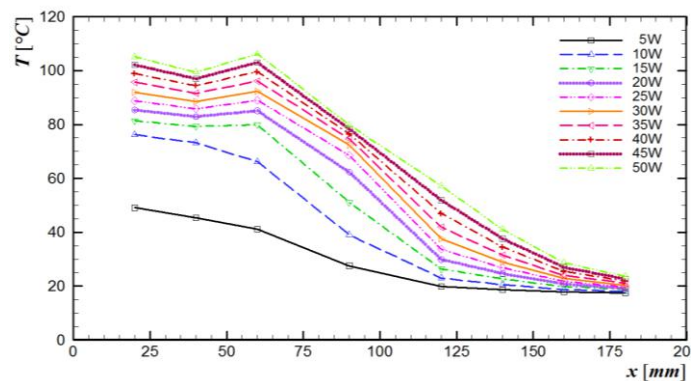


Fig. 7: Temperature distribution versus finned thermosyphon length

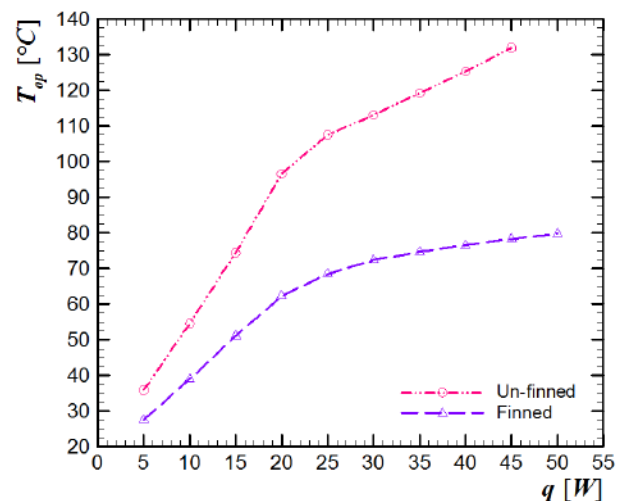


Fig. 8: Operation temperature versus heat load

The operating temperature of the finned thermosyphon in function of the heat load is shown in Fig. 8. Figure 9 illustrates the behavior of the thermal resistance as a function of heat load. Also in these graphs, the results of

un-finned thermosyphon with the same characteristics are presented [13], in order to analyze the effectiveness of the extended surfaces.

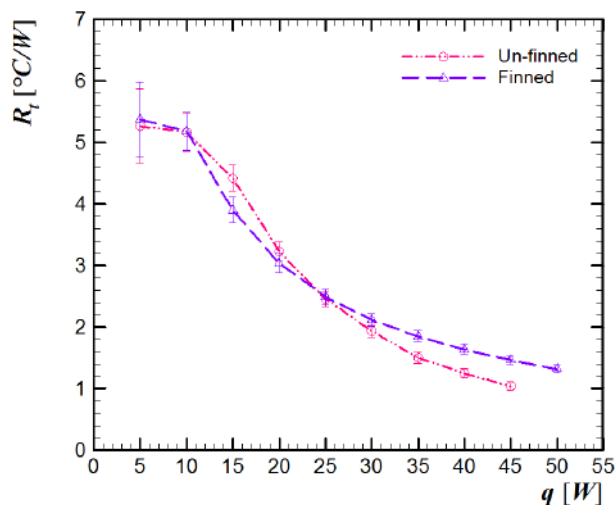


Fig. 9: Thermal resistance versus heat load

For both thermosyphons, the operating temperature increases with the rise of the heat load. Furthermore, the thermal resistances decrease with the increasing heat dissipation in the evaporator. According to the experimental results, the thermal resistance remains similar for the finned and un-finned condenser. Nonetheless, the operating temperature significantly drops, which proves the fins effectiveness. As a result, the finned thermosyphon can operate at higher heat load with a lower operating temperature.

V. CONCLUSION

This paper presented a thermal analysis of a finned thermosyphon for heat exchanger applications. Experimental tests were performed to a heat load from 5 up to 50W at the vertical position. The working fluid was water. As a result of the research, the thermosyphon operated satisfactorily for the tested position. Also, the finned thermosyphon obtained better thermal performance than the un-finned condenser, proving the effectiveness of the fin application.

ACKNOWLEDGEMENTS

Acknowledgments are provided to the Capes, the CNPq, the PROPPG/UTFPR, the DIRPPG/UTFPR, the PPGEM/UTFPR/PG, and the DAMEC/UTFPR/PG.

REFERENCES

[1] A. Akbaszadeh, T. Wadowski, Heat Pipe-based cooling systems for photovoltaic cells under concentrated solar radiation, *Applied Thermal Engineering*, Vol. 16, pp. 81-87, 1996.

[2] D.A. Reay, P.A. Kew, R.J. McGlen, *Heat Pipe: Theory, Design and Applications*, Butterworth-Heinemann, Amsterdam, NED, 2014.

[3] M.B.H. Mantelli, Thermosyphon technology for industrial applications, Chapter 11, In: Vasiliev L.L. and Kakaç S. (Eds.), *Heat pipes and solid sorption transformations: fundamentals and practical applications*. CRC Press, Boca Raton, USA, 2013.

[4] S.W. Chi, *Heat Pipe Theory and Practice: A Sourcebook*, Hemisphere Publishing Corporation, Washington, 1976.

[5] G.P. Peterson, *An Introduction to Heat Pipes: Modeling, Testing and Applications*, (Thermal Management of Microelectronic and Electronic System Series). Wiley-Interscience, New York, 1994.

[6] A. Faghri, "Heat Pipes: Review, Opportunities and Challenges", *Frontiers in Heat Pipes*, Vol. 5, pp 01-48, 2014.

[7] V.M. Aguiar, Influence of filling ratio and inclination angle on thermal performance of thermosyphons, Graduation work, Federal University of Technology – Paraná, Ponta Grossa, Brazil (in Portuguese).

[8] L. Krambeck, F.B. Nishida, P.H.D. Santos, T. Antonini Alves, Configurations of phosphor bronze meshes in heat pipes: an experimental analysis of thermal performance, *International Journal of Advanced Engineering Research and Science*, Vol. 2, pp 11-14, 2015.

[9] G.M. Russo, L. Krambeck, F.B. Nishida, P.H.D. Santos, T. Antonini Alves, Thermal performance of thermosyphon for different working fluids, *Engenharia Térmica*, Vol. 15, pp 3-8, 2016.

[10] P.H.D. Santos, K.A.T. Vicente, L.S. Reis, L.S. Marquardt, T. Antonini Alves, Modeling and experimental tests of a copper thermosyphon, *Acta Scientiarum. Technology (online)*, Vol. 39, pp 59-68, 2017.

[11] J.P. Holman, *Experimental Methods for Engineers*. McGraw-Hill, New York, USA, 2011.

[12] T.L. Bergman, A.S. Lavine, F.P. Incropera, D.P. DeWitt, *Fundamentals of Heat and Mass Transfer*, John Wiley & Sons., New York, USA, 2011.

[13] L. Krambeck, F.B. Nishida, V.M. Aguiar, P.H.D. Santos, T. Antonini Alves, Thermal performance evaluation of different passive devices for electronics cooling, *Thermal Science*, in press, 2018.